Available online at www.sciencedirect.com
SCIENCE DIRECT®
Journal of Molecular Catalysis A: Chemical 218 (2004) 91–100
JOURNAL OF MOLECULAR CATALYSIS A: CHEMICAL
www.elsevier.com/locate/molcata

Degenerate propene metathesis on Mo-alkylidene centres of molybdena–alumina catalyst—a DFT study

Jaroslaw Handzlik*

Institute of Organic Chemistry and Technology, Cracow University of Technology, Warszawska 24, PL 31-155 Cracow, Poland

Received 29 January 2004; received in revised form 1 April 2004; accepted 3 April 2004

Available online 12 May 2004

Abstract

Degenerate propene metathesis proceeding on Mo-alkylidene centres situated on alumina is theoretically investigated, applying the B3LYP functional. The Gaussian 98 package is used. The present results are compared with previous ones, concerning the productive metathesis. It is concluded that on the Mo-ethylidene sites the degenerate metathesis is preferred over the productive one. This is not the case for the Mo-methylidene centres, however. According to the calculations, the population of the Mo-ethylidene centres should be higher than in the case of the Mo-methylidene ones and the formers are the predominant chain carriers for the degenerate metathesis. The relative energies of mono-methyl substituted, as well as, 1,2- and 1,3-dimethyl substituted trigonal bipyramidal and square pyramidal molybdacyclobutanes are also compared.

Keywords: Molybdena–alumina; Propene metathesis; Degenerate; DFT; Molybdacyclobutane; Methylidene; Ethylidene; Gaussian

1. Introduction

A commonly accepted carbene mechanism of olefin metathesis involves metal-alkylidene complexes and metallacyclobutane intermediates [1]. Originally proposed for homogeneous systems, the carbene mechanism has been adopted to the heterogeneous olefin metathesis [2–17]. In Fig. 1, a mechanism of productive propene metathesis is presented.

Productive olefin metathesis is accompanied by so-called degenerate (or non-productive) metathesis [2,14–18]. In the case of degenerate propene metathesis, the two schemes presented in Fig. 2 should be considered. Both in the case of the productive and degenerate metathesis, the same active centres, [M]=CH_2 and [M]=$CHCH_3$, are involved in the reaction mechanism.

It was shown for heterogeneous molybdena systems that the degenerate metathesis proceeds faster than the productive one [14–18]. The relative rate of the degenerate metathesis depends on the kind of the support applied [15]. For instance, on molybdena–silica systems the rate of degenerate metathesis of propene is about 20–90 times faster than the rate of the productive one, while on analogous molybdena–alumina catalysts the rate of the degenerate metathesis is only 3–4 times faster [15].

There are several experimental evidences indicating that the predominant chain carrier for the degenerate metathesis of propene on heterogeneous molybdena catalysts is [Mo]=$CHCH_3$ rather than [Mo]=CH_2 [2,14–17]. This is explained by different reactivity depending on the orientation of propene molecule to Mo-alkylidene centres [14–17]. In the case of the productive metathesis, it was proposed that the reaction of propene with [Mo]=$CHCH_3$ is a rate-determining step, so the population of [Mo]=$CHCH_3$ sites is increased [14]. Thus, the productive and degenerate metathesis are competitive reactions of propene with Mo-ethylidene centres, however the latter reaction does not change the population of the [Mo]=$CHCH_3$ centres. The faster rate of the degenerate metathesis, in comparison to the productive one, was explained by higher reactivity of the molybdacyclobutane intermediates with methyl substituents in 1,3 positions, comparing to the 1,2-substituted molybdacyclobutanes [15] (see Figs. 1 and 2).

In the previous work [19], a detailed theoretical study of productive propene metathesis proceeding on

* Tel.: +48-12-6282761; fax: +48-12-6282037.
E-mail address: jhandz@usk.pk.edu.pl (J. Handzlik).

1381-1169/$ – see front matter © 2004 Elsevier B.V. All rights reserved.
doi:10.1016/j.molcata.2004.04.005

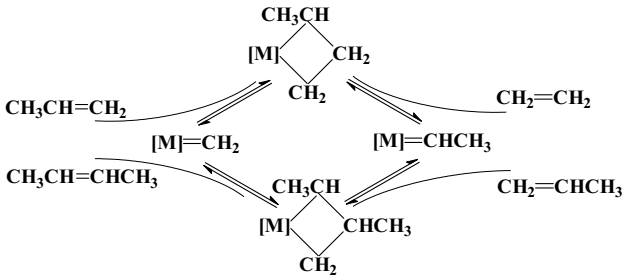

Fig. 1. Mechanism of productive propene metathesis.

molybdena–alumina catalyst was carried out, applying the cluster model approach. The obtained results predicted, in agreement with [14], that a reaction of propene with Mo-ethylidene centre, leading to Mo-methylidene and 2-butene is a slower step than the pathway from propene and [Mo]=CH_2 to ethene and [Mo]=$CHCH_3$ [19]. In the present work, complementary DFT investigations of degenerate metathesis of propene are reported. Details of the reaction mechanism and energetic aspects are discussed. The present results are compared with the previous ones concerning the productive propene metathesis.

2. Computational

Calculations were carried out with the Gaussian 98 program [20]. The hybrid B3LYP functional [21,22] with the LANL2DZ basis set was used. This basis includes the Hay–Wadt effective core potential plus double-zeta basis [23] (applied for Mo and Al) and Dunning–Huzinaga valence double-zeta basis [24] on the first row (applied for C, H and O).

The cluster approach was applied to model the surface active sites of propene metathesis. Alumina is represented by a small cluster with formula $Al_2(OH)_6$, in which two hydroxyl groups are replaced by Mo site. This model was used in the previous works [19,25–27] and its correctness was discussed and verified [19,26].

All the structures were fully optimised to make localisation of transition states easier. The optimised geometry of the alumina part of the models is hardly changed, when going from one structure to another [19]. The Berny algorithm with redundant internal coordinates was employed [28]. Harmonic vibration frequencies were calculated for each structure to confirm the potential energy minimum or the transition state involved, and, to obtain the zero-point energy (ZPE) values. All presented energies are ZPE corrected. The obtained transition structures were additionally verified by the IRC calculations [29,30].

3. Results and discussion

3.1. Models of [Mo]=CH_2 and [Mo]=$CHCH_3$ sites

Models of monomeric Mo^{VI} methylidene (**1**) and ethylidene centres (**2s**, **2a**) on alumina were described in the previous works [19,26,27]. In the latter case, two rotational isomers can be distinguished, the *syn* rotamer (**2s**) and the *anti* one (**2a**). The former one is a little more stable [19]. The proposed Mo-alkylidene centres possess pseudo-tetrahedral structure with one oxo ligand and other two oxygens connecting the Mo centre with alumina. Thus, the geometry of the Mo centre is analogous to the very effective four-coordinate Mo(NAr)(CHR)(L_2) Schrock catalysts [31,32], taking into account that the O= ligand in the studied structures corresponds to the NAr one in the Schrock complexes. The geometry details [19,27] of the proposed models of the active sites are well consistent with both experimental data [31] and previous theoretical results [33–36] concerning molybdenaalkylidene complexes.

To the best of my knowledge, there is no available spectroscopic data concerning the surface Mo-alkylidene complexes on alumina. However, some comparisons of the present models with similar systems are possible. It was previously shown [19] that the calculated wavenumbers of the C–H stretching vibrations of the alkylidene moiety of the models are in a very good agreement with the experimental data concerning surface Mo-methylidene and Mo-ethylidene complexes on silica [10,11]. For instance, the four calculated and scaled wavenumbers of the *syn*-Mo-ethylidene centre are in the range 2861–2991 cm^{-1}, while the corresponding experimental values are between 2850 and 2985 cm^{-1}. In Table 1, other theoretically predicted wavenumbers of harmonic vibrations of the *syn*-Mo-ethylidene (**2s**) are listed. The same scaling factor as in the previous work [19] is used to recalculate the wavenumbers. The calculated and scaled frequencies of the CH_3 deformation (1357–1435 cm^{-1}, Table 1) are very close, within 20 cm^{-1}, to the bands observed in a very recent reflectance absorbance IR spectroscopy study

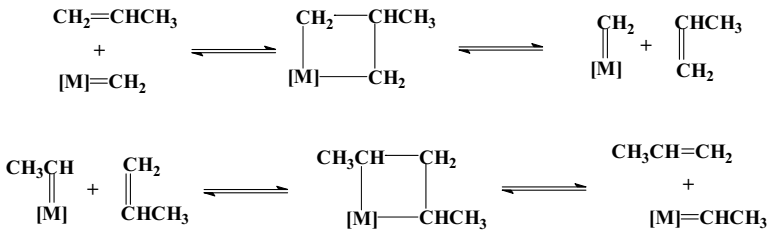

Fig. 2. Degenerate propene metathesis.

Table 1
Selected wavenumbers of the harmonic vibrations calculated for the *syn*-Mo-ethylidene centre

Calculated frequency (cm^{-1})	Scaled frequency (cm^{-1})[a]	Mode
1508	1435	Antisymmetric CH_3 deformation
1504	1431	Antisymmetric CH_3 deformation
1426	1357	Symmetric CH_3 deformation
1290	1228	CH deformation + CH_3 deformation + Mo=C stretch + C–C stretch
1129	1074	C–C stretch + Mo=C stretch + CH_3 deformation
1019	970	CH_3 deformation
989	941	Mo=O stretch + CH deformation
947	901	CH deformation + CH_3 deformation
796	757	CH deformation + antisymmetric Mo–O stretch + antisymmetric Al–O stretch
677	644	CH deformation
647	616	Mo=C stretch + Mo=C–C deformation

[a] 0.9516 scaling factor was applied.

of ethylidene on a molybdenum carbide surface [37]. The frequency of the Mo=O stretching mode, which is a little mixed with the C–H deformation is similar to the results obtained by Raman spectroscopy for MoO_3/Al_2O_3 systems [38–44]. According to the present calculations, the Mo=C stretching vibration is strongly mixed with the C–C stretching one, as well as with the CH_3, CH and Mo=C–C deformation modes. It was reported for W–alkylidyne complexes that the W≡C stretching vibration is coupled with the C–C stretching and CH_3 deformation modes [45]. The calculated

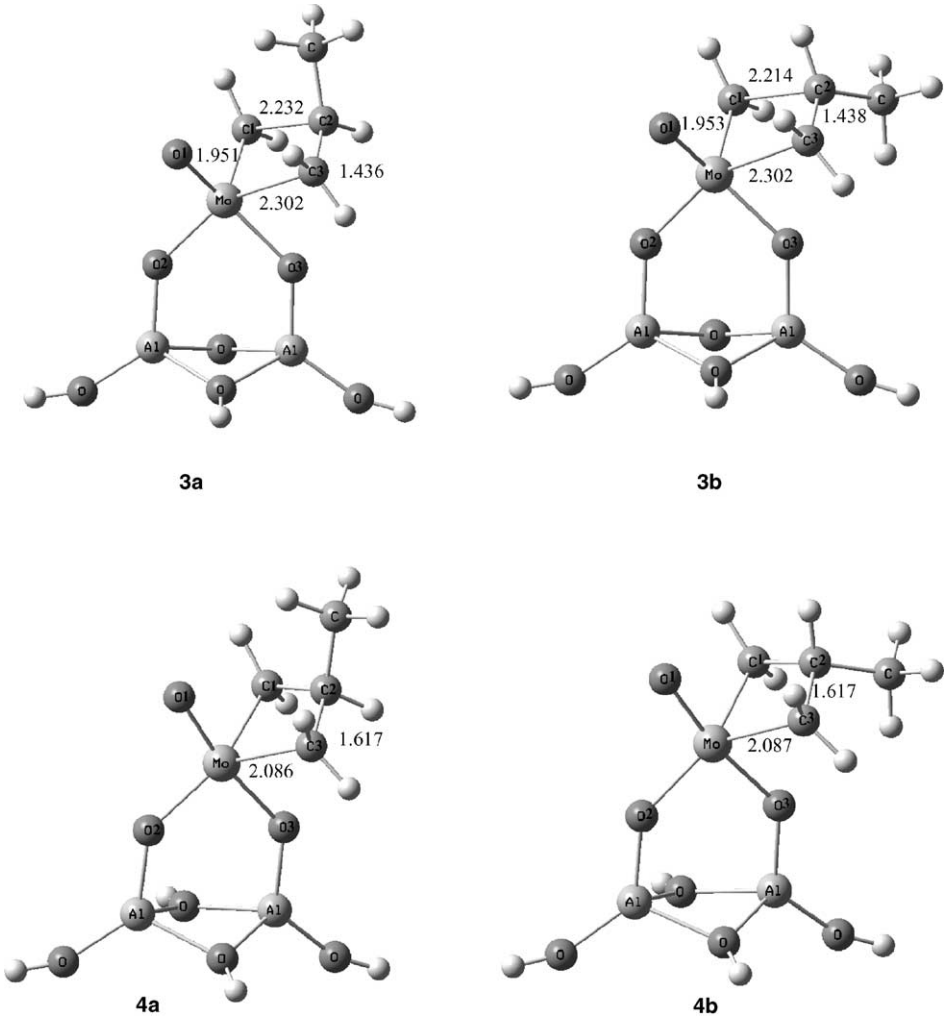

Fig. 3. Degenerate propene metathesis on the Mo-methylidene centre **1**. Optimised structures of the transition states (**3a** and **3b**) and the corresponding TBP molybdacyclobutanes (**4a** and **4b**). Bond lengths are given in Å.

1228 and 1074 cm^{-1} wavenumbers are also not very different from the band detected for cyclobutylidene on β-Mo_2C (1130 cm^{-1}) [46].

3.2. Mechanism of degenerate metathesis of propene

When degenerate metathesis reaction proceeds via Mo-methylidene centre, propene molecule can add to the carbene bond in two ways that differ in orientation of the methyl group. The calculated geometries of the corresponding transition states (**3a** and **3b**) are shown in Fig. 3. They have nearly flat rings with the predicted Mo–C1–C3–C2 dihedral angles of about −179 and 173°, respectively. The localised transition states lead to molybdacyclobutane intermediates (**4a** and **4b**, Fig. 3) with entirely flat rings and trigonal bipyramidal geometry (TBP). The O2, C1 and C3 atoms form the base of the trigonal bipyramid, whereas the O1 and O3 atoms are the vertexes. Both the obtained transition structures and the molybdacyclobutane intermediates have geometries analogous to the corresponding structures previously calculated for productive propene metathesis [19].

Decomposition of the molybdacyclobutane intermediate to Mo-methylidene centre and propene is the next step of degenerate metathesis. Thus, structures **4a** and **4b** can decompose to [Mo]=$C3H_2$ and $C1H_2$=C2H–CH_3. Because of C_s symmetry of **4a** and **4b**, this pathway is identical with the pathway of the reverse reaction, leading via transition states **3a** and **3b** to [Mo]=$C1H_2$ (**1**) and $C3H_2$=C2H–CH_3.

Analogously as in the case of productive propene metathesis [19], the TBP molybdacyclobutane can rearrange to the square pyramidal (SP) one. In Fig. 4, the calculated structures of the SP intermediates **6a** and **6b**, as well as the corresponding transition states **5a** and **5b** are presented. O2, O3, C1 and C3 atoms form the base of the square pyramid in **6a** and **6b**, whereas O1 atom is the vertex. According to both previous results [19,27] and present investigations, the SP molybdacyclobutanes can decompose to the respective

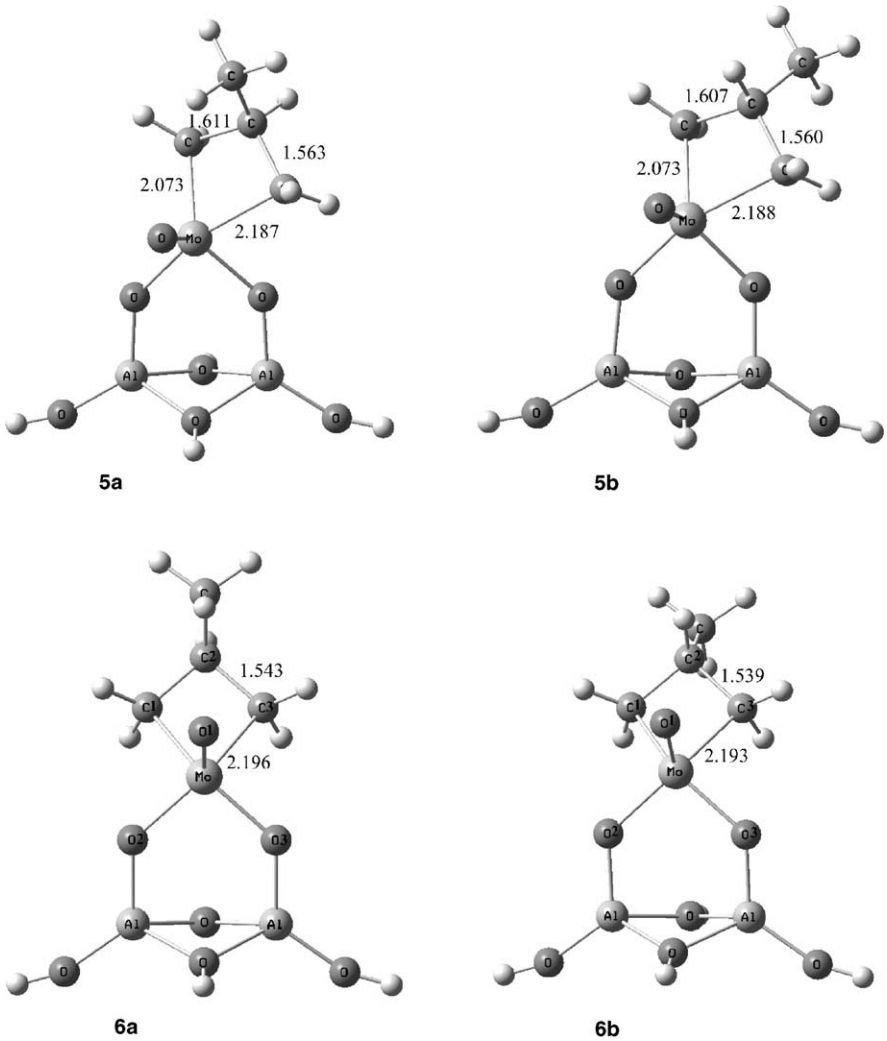

Fig. 4. Degenerate propene metathesis on the Mo-methylidene centre **1**. Optimised structures of the transition states (**5a** and **5b**) and the corresponding SP molybdacyclobutanes (**6a** and **6b**). Bond lengths are given in Å.

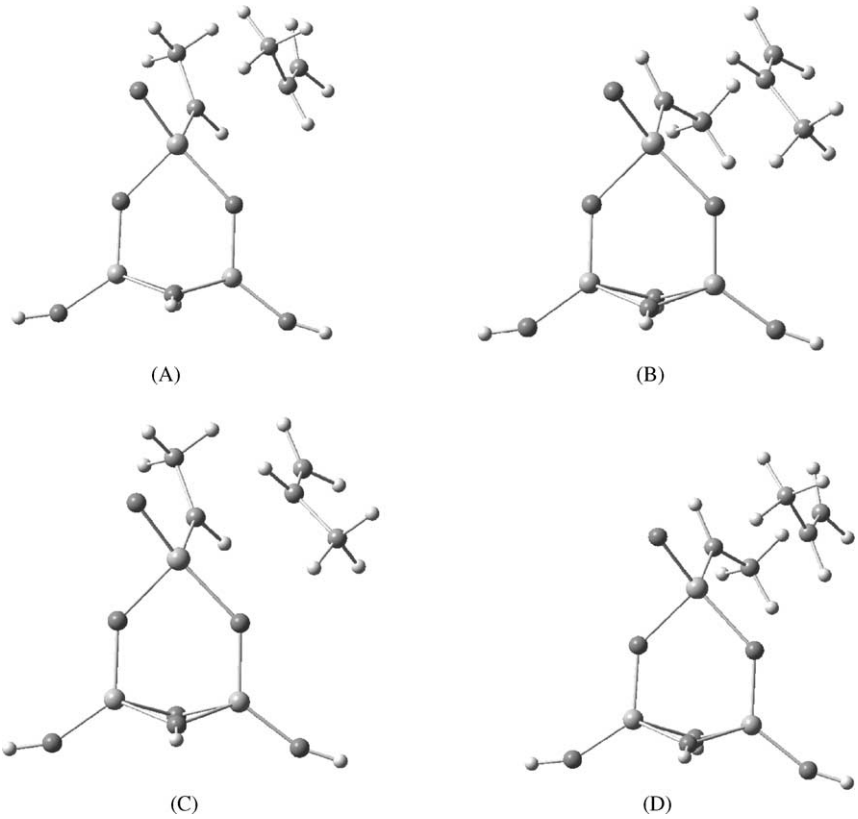

Fig. 5. Four possibilities of propene addition to the Mo-ethylidene centre during the degenerate metathesis.

Mo-methylidene complexes and propene only via the TBP intermediate. This is also consistent with suggestions of Schrock and co-workers [31] and other theoretical results [34].

In Fig. 5, possible orientations of attacking propene molecule towards the Mo-ethylidene centres are shown. Only degenerate metathesis is taken into account. Considering A and B orientations, we can notice that the same rotational isomer of [Mo]=$CHCH_3$ will be reproduced after one catalytic cycle. There are also two other possibilities: the *anti* rotamer can be obtained from the *syn* one (Fig. 5, C) and vice versa (Fig. 5, D).

Geometries of the transition states (**7s** and **7a**) of propene addition to the *syn*- and *anti*-Mo-ethylidene complex (A and B cases) together with the predicted structures of the corresponding TBP molybdacyclobutanes (**8s** and **8a**) are presented in Fig. 6. The calculated geometries are fully analogous to those obtained for the reactions proceeding on the Mo-methylidene centre. The **8s** and **8a** TBP intermediates have the C_s symmetry, so the decomposition pathway is identical to the reverse reaction **8s**(**8a**) → **2s**(**2a**) + C_3H_6. The mentioned metathesis reactions can be accompanied by rearrangements of the TBP molybdacyclobutanes via transition states **9s** and **9a** to the SP intermediates **10s** and **10a** (Fig. 7).

Propene addition in C manner to the *syn*-Mo-ethylidene centre **2s** (Fig. 5) leads to TBP intermediate **12**, via transition state **11** (Fig. 8). Further decomposition of **12** to the *anti*-Mo-ethylidene complex **2a** and propene involves transition state **13**. Considering the reverse transformation, i.e. **2a** + C_3H_6 → **12** → **2s** + C_3H_6, one can notice that it represents the D case of propene addition (Fig. 5). Rearrangement of the TBP intermediate **12** to the SP molybdacyclobutane **15**, which is competitive to the ring decomposition, involves transition state **14** (Fig. 8).

In Fig. 9, an energy diagram of degenerate propene metathesis on the Mo-methylidene centre **1** is shown. The pathways on the left and right side of the diagram concern the two possible orientations of propene molecule during its addition to the Mo=C bond. It is seen that both sides of the diagram are almost identical.

It was proposed [16,17] that the reactivity of the [Mo]=CH_2 site depends strongly on the orientation of propene molecule and propene addition leading to the productive metathesis is preferred. So, it is a little surprising that the predicted activation barrier of propene addition to **1** in non-productive way is practically the same as for the productive metathesis leading to the **2s** centre—in the latter case the value is even 1 kJ mol^{-1} higher [19]. However, in the case of the degenerate metathesis, the transformation of the TBP molybdacyclobutane (**4a**, **4b**) to the SP one (**6a**, **6b**) proceeds easier than decomposition of the former to the Mo-methylidene centre **1** and ethene (Fig. 9). Taking into account a much lower energy of the SP intermediate, comparing to the TBP one, it can be predicted that degenerate propene metathesis causes a rearrangement of a portion of the active Mo-methylidene sites into much more stable and

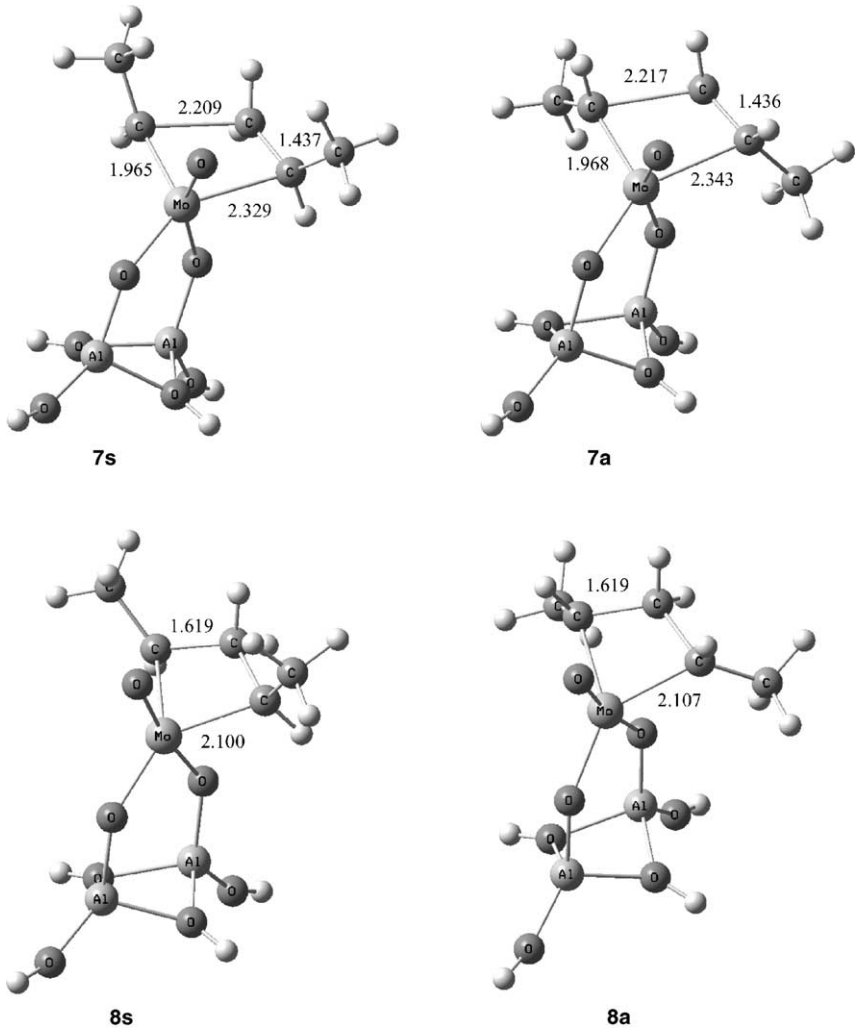

Fig. 6. Degenerate propene metathesis on the Mo-ethylidene centres **2s** and **2a** (A and B cases). Optimised structures of the transition states (**7s** and **7a**) and the corresponding TBP molybdacyclobutanes (**8s** and **8a**). Bond lengths are given in Å.

less active SP molybdacyclobutanes. On the other hand, in the case of the productive metathesis, the calculated energy barrier of the TBP molybdacyclobutane decomposition to Mo-ethylidene centre and ethene is ca. 10 kJ mol^{-1} lower (B3LYP/LANL2DZ) than the barrier of its undesired transformation to the stable SP intermediate [19]. This is the reason that, according to the present calculations, degenerate propene metathesis on Mo-methylidene centre does not seem to be preferred over the productive one.

Propene addition in A manner to the *syn*-Mo-ethylidene centre **2s** (Fig. 5, A) has about 3 kJ mol^{-1} lower activation energy (Fig. 10) than in the case of the reaction proceeding on the Mo-methylidene centre (Fig. 9). What is important, in the former case, the decomposition of the TBP molybdacyclobutane to metathesis products is preferred by about 11 kJ mol^{-1} over the undesired transformation to the SP intermediate. The predicted energy barrier of propene addition in B manner to the *anti*-Mo-methylidene centre (Fig. 5, B) is about 8 kJ mol^{-1} higher than in the case A (Fig. 10).

When propene reacts with *syn*-Mo-ethylidene site in such a way that the *anti* rotamer is obtained (Fig. 5, C), the calculated barrier of this addition is 6 kJ mol^{-1} higher than in the case A (Fig. 10). The reverse reaction, transforming the *anti*-Mo-ethylidene centre into the *syn* one (the D case) occurs a little easier. Both in the cases C and D, the second metathesis step, i.e. decomposition of the TBP molybdacyclobutane is kinetically preferred over the conversion of the TBP intermediate to the SP one (Fig. 10). Because the *anti*-Mo-ethylidene centre is less stable and can be easily transformed via degenerate metathesis into the *syn* rotamer and the pathway leading to the *syn*-Mo-ethylidene centre via productive propene metathesis on **1** is kinetically preferred over the competitive pathway leading to the *anti* rotamer [19], one can expect the population of the *syn* species being higher than that of the *anti* one.

It was previously shown for productive propene metathesis proceeding on the Mo-ethylidene centre that the transition state of decomposition of the TBP molybdacyclobutane to the Mo-methylidene centre and 2-butene

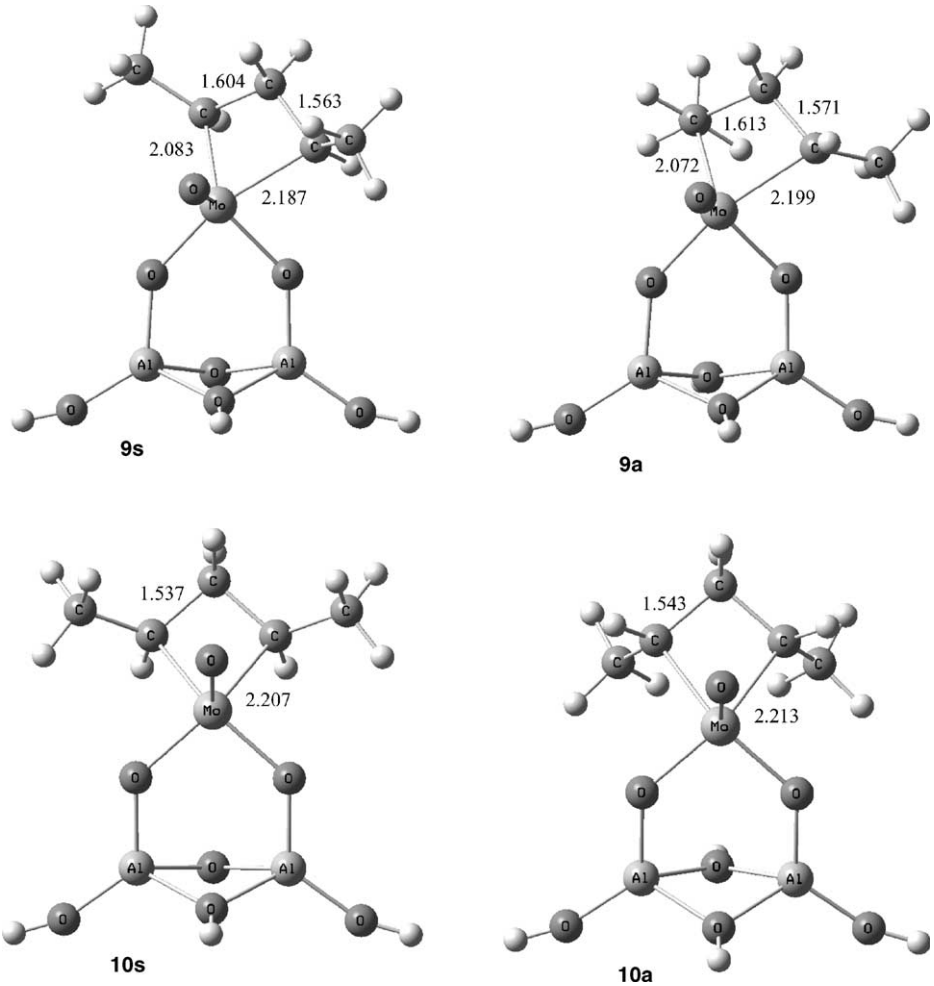

Fig. 7. Degenerate propene metathesis on the Mo-ethylidene centres **2s** and **2a** (A and B cases). Optimised structures of the transition states (**9s** and **9a**) and the corresponding SP molybdacyclobutanes (**10s** and **10a**). Bond lengths are given in Å.

is the highest point on the pathway, including conversion to the SP intermediate [19]. Energy of this TS is over $50\,kJ\,mol^{-1}$ (B3LYP/LANL2DZ) higher than energy of the Mo-ethylidene and propene. Comparing those results with the calculated pathways of the degenerate metathesis (Fig. 10), especially the cases A and C, it is clear that the degenerate metathesis of propene on the Mo-ethylidene centres proceeds faster than the productive metathesis. It is consistent with the reported experimental results for heterogeneous molybdena catalysts [14–18].

According to the calculations [19], during the productive propene metathesis, the Mo-methylidene centres change to the Mo-ethylidene ones easier than in the case of the vice versa process. Thus, the population of the Mo-ethylidene species should be higher than that of the Mo-methylidene one and the former is the predominant chain carrier for the degenerate metathesis. This statement is consistent with experimental results obtained from investigations using deuterium-labelled olefins [14–17]. As was concluded above, the dominant species should be the *syn*-Mo-ethylidene one.

It was postulated [15] that the relative rates of the productive and degenerate metathesis are controlled by activities of the molybdacyclobutane intermediates. The results of the previous [19] and present calculations confirm this statement, however a more detailed explanation is given. For the reaction proceeding on the Mo-ethylidene centre, both calculated energy of the TBP intermediate and the activation energy of its decomposition to the metathesis products are higher for the productive metathesis than for the degenerate one. What is also important, in the former case, the undesired transformation of the TBP molybdacyclobutane to the SP one is kinetically preferred in comparison to the conversion of the TBP intermediate to the metathesis products. This is not true, however, in the case of the degenerate metathesis (Fig. 10).

3.3. Relative energies of molybdacyclobutane intermediates

In Fig. 11, the relative energies of mono-methyl substituted molybdacyclobutanes are shown, whereas in Fig. 12, the values for dimethyl substituted ones are presented. The

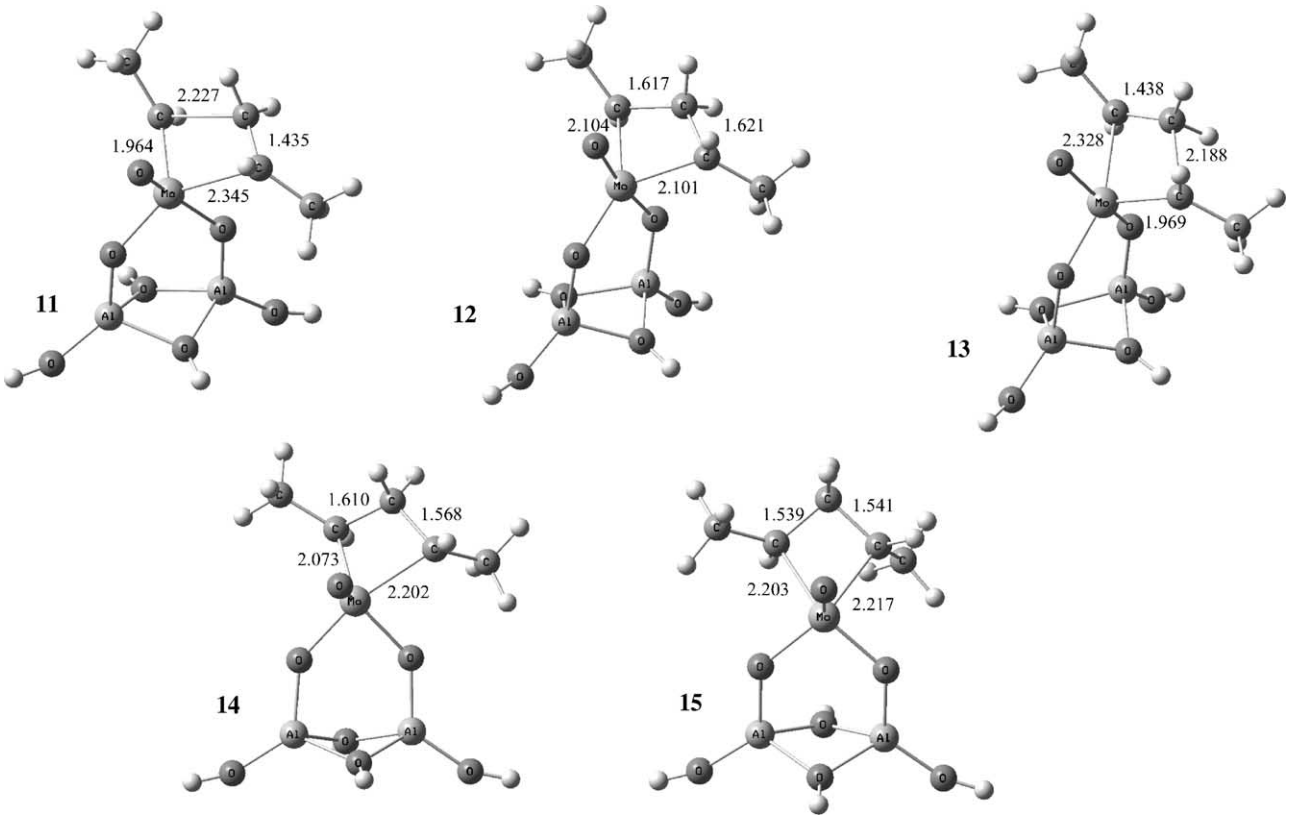

Fig. 8. Degenerate propene metathesis on the Mo-ethylidene centres **2s** and **2a** (C and D cases). Optimised structures of the transition states (**11**, **13**) leading to the BP molybdacyclobutane **12**, as well as the geometry of the transition structure **14** and the corresponding SP molybdacyclobutane **15**. Bond lengths are given in Å.

energies of the intermediates involved in productive metathesis are taken from the previous study [19]. As one can see, the energy orders for the TBP and SP intermediates are not the same. In the case of the mono-methyl substituted rings, the TBP complexes with the methyl substituent in position 2, being intermediates of the degenerate metathesis, have a little higher energies than the molybdacyclobutanes with the substituent in position 1.

1,3-Dimethyl substituted TBP molybdacyclobutanes that are intermediates of degenerate metathesis are generally more stable than the 1,2-dimethyl substituted ones. The order of the calculated relative energies of the TBP intermediates does not match exactly the order of the energy barriers of the corresponding reactions of propene addition to the Mo=C bond. However, comparing the energy diagrams (Fig. 10 and the results published in [19]) with the relative energies of the TBP intermediates, one can conclude that despite of the complex kinetics of the process, approximate predictions of the reactivity can be done on the basis of the TBP molybdacyclobutane energies.

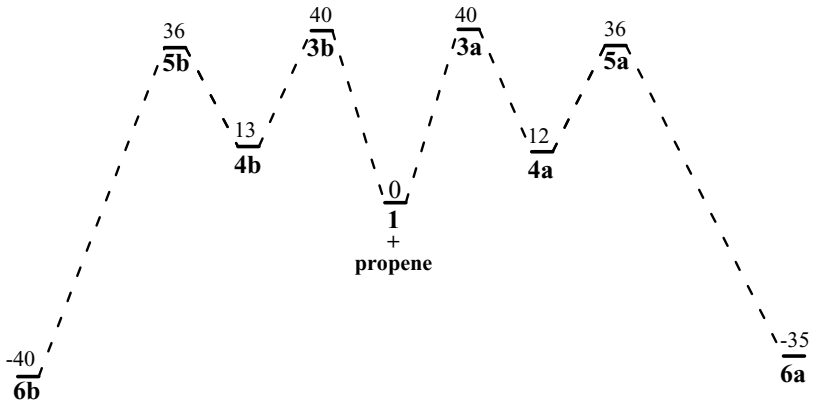

Fig. 9. Energy diagram (kJ mol^{-1}) of degenerate propene metathesis on the Mo-methylidene centre **1**.

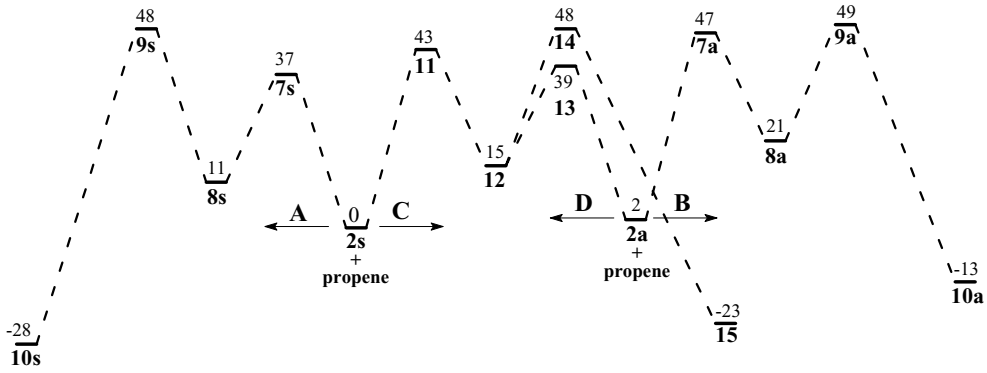

Fig. 10. Energy diagram (kJ mol^{-1}) of degenerate propene metathesis on the Mo-ethylidene centres **2s** and **2a**. A, B, C and D refer to the four possibilities shown in Fig. 5.

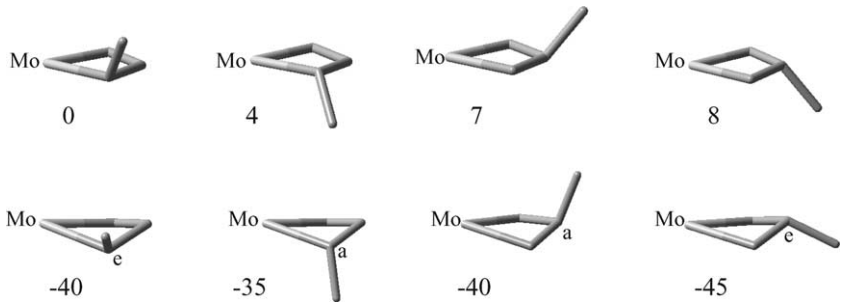

Fig. 11. The relative energies (kJ mol^{-1}) of the mono-methyl substituted molybdacyclobutanes.

In the case of the SP molybdacyclobutanes, the puckered conformation of the ring allows to minimise the repulsion between the methyl substituents. They adopt pseudo-axial or pseudo-equatorial positions. For the mono-methyl substituted intermediates, the equatorial position is preferred (Fig. 11). Stereoselectivity of olefin metathesis is often explained on the basis on favoured stereo conformation of alkyl substituted molybdacyclobutanes [14–17,47]. The molybdacyclobutane leading to the *trans* product have the 1,2-methyl substituents in equatorial positions, whereas the methyl groups in the molybdacyclobutane leading to the *cis* configuration adopt one equatorial and one axial position. The latter intermediate has higher energy than the former one (Fig. 12). There is also a second possible structure of molybdacyclobutane leading to the *trans* product. This structure has both substituents in axial positions and its energy is 10 kJ mol^{-1} higher than in the case of the intermediate with the methyl groups in equatorial position (Fig. 12). The equatorial positions of the substituents in the ring are also favoured for the 1,3-dimethyl-substituted molybdacyclobutanes involved in the degenerate metathesis. In contrast to the corresponding BP structures, the 1,3-SP intermediates did not have lower energies than the 1,2-dimethyl substituted ones.

Generally, for the process studied, the kinetic predictions should rather be based on the BP intermediate energies than on the SP molybdacyclobutane ones, because the latter structures do not rearrange directly to the metathesis products.

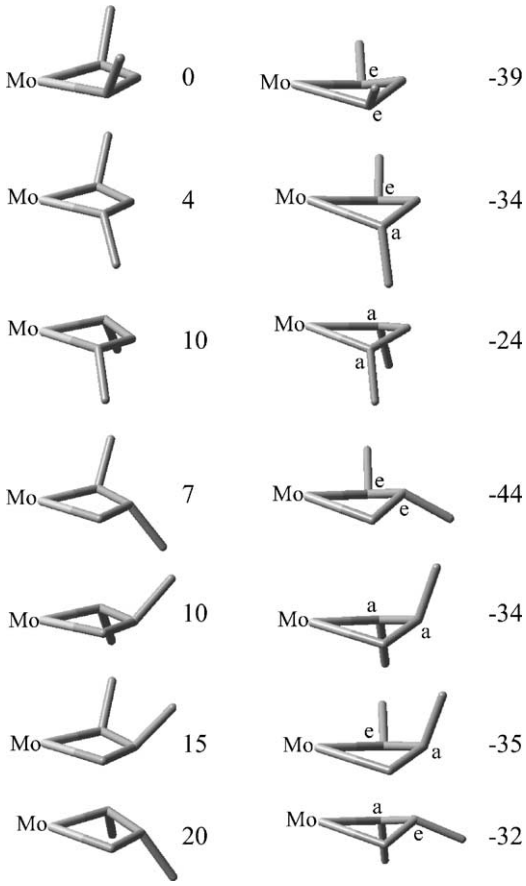

Fig. 12. The relative energies (kJ mol^{-1}) of the dimethyl substituted molybdacyclobutanes.

4. Conclusions

The calculated mechanism of the degenerate propene metathesis proceeding on Mo-alkylidene centres situated on alumina is analogous to the previously predicted for the productive metathesis. On the basis of the relative energies of the intermediates and the transition states, it is concluded that on the Mo-ethylidene centres the degenerate metathesis is favoured over the productive one. This is not true, however, in the case of the Mo-methylidene sites.

It is also predicted that the population of the Mo-ethylidene centres is higher than in the case of the Mo-methylidene ones and the formers are the predominant chain carriers for the degenerate metathesis. These statements are consistent with the reported experimental results.

Acknowledgements

Computing resources from Academic Computer Centre CYFRONET UMM (SGI Origin 2800 computer, grant No. KBN/SGI_ORIGIN_2000/PK/109/1999) are gratefully acknowledged. The author thanks Prof. P.H. McBreen for discussion and access to his unpublished results.

References

[1] J.-L. Hérisson, Y. Chauvin, Makromol. Chem. 141 (1971) 161.
[2] K.J. Ivin, J.C. Mol, Olefin Metathesis and Metathesis Polymerization, Academic Press, London, 1997.
[3] R.H. Grubbs, S.J. Swetnick, J. Mol. Catal. 8 (1980) 25.
[4] M.F. Farona, R.L. Tucker, J. Mol. Catal. 8 (1980) 85.
[5] J.R. McCoy, M.F. Farona, J. Mol. Catal. 66 (1991) 51.
[6] F. Kapteijn, H.L.G. Bredt, E. Homburg, J.C. Mol, Ind. Eng. Chem. Prod. Res. Dev. 20 (1981) 457.
[7] V.G. Gomes, O.M. Fuller, AIChE J. 42 (1996) 204.
[8] Y. Iwasawa, H. Kubo, H. Hamamura, J. Mol. Catal. 28 (1985) 191.
[9] B.N. Shelimov, I.V. Elev, V.B. Kazansky, J. Mol. Catal. 46 (1988) 187.
[10] K.A. Vikulov, I.V. Elev, B.N. Shelimov, V.B. Kazansky, J. Mol. Catal. 55 (1989) 126.
[11] K.A. Vikulov, B.N. Shelimov, V.B. Kazansky, J. Mol. Catal. 65 (1991) 393.
[12] K.A. Vikulov, B.N. Shelimov, V.B. Kazansky, J. Mol. Catal. 72 (1992) 1.
[13] K.A. Vikulov, B.N. Shelimov, V.B. Kazansky, J.C. Mol, J. Mol. Catal. 90 (1994) 61.
[14] K. Tanaka, K. Tanaka, H. Takeo, C. Matsumura, J. Am. Chem. Soc. 109 (1987) 2422.
[15] K. Tanaka, in: Y. Ímamoglu (Ed.), Olefin Metathesis and Polymerization Catalysts, NATO ASI Series C326, Kluwer Academic Publishers, Dordrecht, 1990, p. 303.
[16] K. Tanaka, Appl. Catal. A 188 (1999) 37.
[17] K. Tanaka, N. Takehiro, J. Mol. Catal. A 141 (1999) 39.
[18] K. Tanaka, K. Tanaka, J. Chem. Soc., Chem. Commun. (1984) 748.
[19] J. Handzlik, J. Catal. 220 (2003) 23.
[20] M.J. Frisch, G.W. Trucks, H.B. Schlegel, G.E. Scuseria, M.A. Robb, J.R. Cheeseman, V.G. Zakrzewski, J.A. Montgomery, R.E. Stratmann, J.C. Burant, S. Dapprich, J.M. Millam, A.D. Daniels, K.N. Kudin, M.C. Strain, O. Farkas, J. Tomasi, V. Barone, M. Cossi, R. Cammi, B. Mennucci, C. Pomelli, C. Adamo, S. Clifford, J. Ochterski, G.A. Petersson, P.Y. Ayala, Q. Cui, K. Morokuma, P. Salvador, J.J. Dannenberg, D.K. Malick, A.D. Rabuck, K. Raghavachari, J.B. Foresman, J. Cioslowski, J.V. Ortiz, A.G. Baboul, B.B. Stefanov, G. Liu, A. Liashenko, P. Piskorz, I. Komaromi, R. Gomperts, R.L. Martin, D.J. Fox, T. Keith, M.A. Al-Laham, C.Y. Peng, A. Nanayakkara, M. Challacombe, P.M.W. Gill, B. Johnson, W. Chen, M.W. Wong, J.L. Andres, C. Gonzalez, M. Head-Gordon, E.S. Replogle, J.A. Pople, Gaussian 98, revision A.11, Gaussian, Inc., Pittsburgh PA, 2001.
[21] A.D. Becke, J. Chem. Phys. 98 (1993) 5648.
[22] P.J. Stevens, J.F. Devlin, C.F. Chabalowski, M.J. Frisch, J. Phys. Chem. 98 (1994) 11623.
[23] P.J. Hay, W.R. Wadt, J. Chem. Phys. 82 (1985) 299.
[24] T.H. Dunning Jr., P.J. Hay, in: H.F. Schaefer III (Ed.), Modern Theoretical Chemistry, vol. 3, Plenum Press, New York, 1976, p. 1.
[25] J. Handzlik, J. Ogonowski, in: A. Corma, F.V. Melo, S. Mendioroz, J.L.G. Fierro (Eds.), Studies in Surface and Science Catalysis, vol. 130, Elsevier, Amsterdam, 2000, p. 1181.
[26] J. Handzlik, J. Ogonowski, J. Mol. Catal. A 175 (2001) 215.
[27] J. Handzlik, J. Ogonowski, J. Mol. Catal. A 184 (2002) 371.
[28] C. Peng, P.Y. Ayala, H.B. Schlegel, M.J. Frisch, J. Comp. Chem. 17 (1996) 49.
[29] C. Gonzalez, H.B. Schlegel, J. Chem. Phys. 90 (1989) 2154.
[30] C. Gonzalez, H.B. Schlegel, J. Phys. Chem. 94 (1990) 5523.
[31] G.C. Bazan, E. Khosravi, R.R. Schrock, W.J. Feast, V.C. Gibson, M.B. O'Regan, J.K. Thomas, W.M. Davis, J. Am. Chem. Soc. 112 (1990) 8378.
[32] J. Feldman, R.R. Schrock, in: S.J. Lippard (Ed.), Progress in Inorganic Chemistry, vol. 39, Wiley, New York, 1991, p. 1.
[33] E. Folga, T. Ziegler, Organometallics 12 (1993) 325.
[34] Y.-D. Wu, Z.-H. Peng, J. Am. Chem. Soc. 119 (1997) 8043.
[35] T.R. Cundari, M.S. Gordon, J. Am. Chem. Soc. 113 (1991) 5231.
[36] T.R. Cundari, M.S. Gordon, Organometallics 11 (1992) 55.
[37] P.H. McBreen, Private communication.
[38] H. Jeziorowski, H. Knözinger, J. Phys. Chem. 83 (1979) 1166.
[39] C.C. Williams, J.G. Ekerdt, J.-M. Jehng, F.D. Hardcastle, I.E. Wachs, J. Phys. Chem. 95 (1991) 8791.
[40] D.S. Kim, I.E. Wachs, K. Segawa, J. Catal. 146 (1994) 268.
[41] H. Hu, I.E. Wachs, S.R. Bare, J. Phys. Chem. 99 (1995) 10897.
[42] G. Mestl, T.K.K. Srinivasan, Catal. Rev.-Sci. Eng. 40 (1998) 451.
[43] R. Radhakrishnan, C. Reed, S.T. Oyama, M. Seman, J.N. Kondo, K. Domen, Y. Ohminami, K. Asakura, J. Phys. Chem. B 105 (2001) 8519.
[44] Y.T. Chua, P.C. Stair, I.E. Wachs, J. Phys. Chem. B 105 (2001) 8600.
[45] J. Manna, R.F. Dallinger, V.M. Miskowski, M.D. Hopkins, J. Phys. Chem. B 104 (2000) 10928.
[46] E. Zahidi, H. Oudghiri-Hassani, P.H. McBreen, Nature 409 (2001) 1023.
[47] J.-M. Basset, D. Boutarfa, E. Custodero, M. Leconte, C. Paillet, in: Y. Ímamoglu (Ed.), Olefin Metathesis and Polymerization Catalysts, NATO ASI Series C326, Kluwer Academic Publishers, Dordrecht, 1990, p. 45.